A novel core-shell structured magnetic organic-inorganic nanohybrid involving drug-intercalated layered double hydroxides coated on a magnesium ferrite core for magnetically controlled drug release†

Hui Zhang,* Dengke Pan, Kang Zou, Jing He and Xue Duan

Received 12th November 2008, Accepted 9th February 2009
First published as an Advance Article on the web 20th March 2009
DOI: 10.1039/b820176e

A novel magnetic nanohybrid involving non-steroid anti-inflammatory drug diclofenac (DIC) intercalated Mg–Al layered double hydroxides (LDH) coated on magnesium ferrite particles was assembled *via* a one step coprecipitation self-assembly method. The XRD, FT-IR and ICP measurements reveal that the magnetic nanohybrid consists of both DIC-LDH nanocrystallite and magnesium ferrite phases. The TEM image shows that the magnetic nanohybrid presents well-defined core-shell structure with diameter in the range of 90–150 nm. Compared to pure DIC-LDH, an obviously smaller dimension and less sharp hexagonal morphology of the coated DIC-LDH nanocrystallites in magnetic hybrids is observed due to a heterogeneous nucleation and crystal growth process with the introduction of the magnetic core. The *in vitro* drug release rate of the magnetic nanohybrid was thus enhanced owing to the much smaller size of the coated DIC-LDH nanoparticles on the surface of the magnetic core. However, under an external magnetic field of 0.15 Tesla, the drug release rate of the magnetic nanohybrid decreases dramatically owing to the aggregation of the magnetic nanohybrid particles triggered by non-contact magnetic force. The kinetic data reveal that the release of DIC from the magnetic nanohybrid is controlled by particle diffusion, and the release rate is mainly affected by the particle size and the aggregation extent of the hybrid magnetic particles. Additionally, the obtained nanohybrid has a strong magnetization response, implying the possibility of application in magnetic drug targeting.

Introduction

Recently, a tremendous number of studies concentrated on layered double hydroxides (LDH) have been reported due to their extensive applications as ion-exchange materials, catalysts, additives in polymers, drug and biomolecules carriers.[1,2] The LDH compounds can be represented by a general formula of $[M^{2+}_{1-x}M^{3+}_{x}(OH)_2]^{x+}A^{n-}_{x/n}\cdot mH_2O$ being of supramolecular structural features, where M^{2+} and M^{3+} designate the di- and trivalent cations, A^{n-} refers to the interlayer anions often in the hydrated form associated with the hydroxide layer through electrostatic attraction, hydrogen-bonding and van der Waals interactions, and x ($= M^{3+}/(M^{2+} + M^{3+})$) stands for the layer charge density.[1,2] Owing to their high flexibility in composition and good biocompatibility, numerous LDH materials with intercalated drugs and biomolecules have been prepared *via* anion exchange and coprecipitation methods, mostly expected for used in developing a new class of drug delivery systems.[2–5] In particular, Choy's group,[3] O'Hare's group,[4] Ambrogi *et al.*[6] and Zhang *et al.*[7] have been focusing on various drug–inorganic hybrid materials (drug-LDH). Their studies demonstrate that this kind of micro-reservoir-type system provides clear advantages, such as high drug loading capacity and better biocompatibility, suggesting that these materials may have potential applications as the basis of a novel tunable drug delivery device. However, the use of bulk drug-LDH in drug delivery system especially in targeted drug delivery mechanisms as carriers has been profoundly restricted due to lack of special affinity towards the pathological sites.

To meet the requirement of selective delivery of chemo-therapeutic agents, magnetic drug targeting was proposed by Widder *et al.*[8] for the first time in the 1970s. Magnetic drug targeting allows the concentration of the drugs at a defined target site with the aid of an external magnetic field, thus the released drug can react exclusively with the pathological sites to reduce the side effects and enhance the bioavailability of the drug.[9–13] Typically, magnetic drug targeting systems have three essential elements: the drug, the pharmaceutical carrier and the targeting moiety (magnetic material).[9] Based on this principle, numerous magnetic drug targeted delivery hybrids have been investigated, including starch/Fe_3O_4,[14] liposome/Fe_2O_3,[15] polymer/Fe_3O_4,[16] peptide/Fe_3O_4,[17] active carbon/Fe,[18] silica/Fe_2O_3 or Fe_3O_4,[19] dendrimer/iron oxide[20,21] and so on. Some researchers reported the magnetically controlled drug release from magnetic drug carriers, such as Edelman *et al.*,[22] Hu *et al.*[23] and Vania *et al.*,[24] who had successfully adjusted the drug release of the magnetic drug targeting system by using an alternating current magnetic

State Key Laboratory of Chemical Resource Engineering, Beijing University of Chemical Technology, P.O. Box 98, Beijing 100029, China. E-mail: huizhang67@gst21.com; Fax: +8610-6442 5385; Tel: +8610-6442 5872

† Electronic supplementary information (ESI) available: XRD structural parameters, and rate constants and r2 coefficients obtained from fitting analyses. See DOI: 10.1039/b820176e

field. Furthermore, the modulating of the drug release by using a direct current magnetic field was also proposed by Chen and co-workers.[25,26] All of these works give us some hints that if one can combine the advantages of the LDH and the magnetic particles to fabricate a nanohybrid with slow release and magnetic response properties, a novel targeted drug delivery matrix which carries the drug directly to a specific organ or location in the body under an external magnetic field could be available.

Previously, we reported a novel magnetic solid base catalyst[27] with a CO_3–MgAl LDH layer and a magnetic nanohybrid composite[28] with the 5-aminosalicylate intercalated LDH layer, respectively, over the magnesium ferrite particles, and revealed a plausible core-shell structure for the obtained products. Recently, Carja *et al.*[29] reported a new magnetic composite based on the aspirin intercalated LDH for drug delivery, and their study shows that the magnetic nanoparticles coexist with the fibrous drug particles on the surface of partially aggregated clay-like particles. The above-mentioned studies demonstrate that these LDH-based hybrids are probably a novel type of magnetic targeted drug delivery matrix. However, previous studies only concentrated on the synthesis and characterization of the magnetic drug-LDH nanohybrid, and further systematic studies are urgently necessary. Moreover, to the best of our knowledge, no investigation has been addressed on the controlled release and release mechanism of a magnetic nanohybrid possessing a LDH shell-magnetic core structure under a stable magnetic field.

In the present work, a novel magnetic drug-LDH nanohybrid with well-defined core-shell structure was fabricated through careful control of the mass ratio of magnesium nitrate salt to magnetic materials during the formation of drug-LDH using diclofenac (DIC) as a model drug *via* a one step coprecipitation method. The quite different particle morphology of the DIC-LDH phase on the magnetic cores from the pure DIC-LDH and a possible formation mechanism were reported. Furthermore, *in vitro* drug release behavior of the magnetic nanohybrid was firstly studied under an external magnetic field and the drug release mechanism related to the microstructure of the hybrid is proposed upon proper kinetic models.

Experimental section

Materials

Diclofenac sodium ($C_{14}H_{10}O_2Cl_2NNa$, $pK_a = 4.0$, denoted as DIC-Na) is purchased from Wuhan Yuancheng Technology Development Co., Ltd, which is used as received. Other reagents are all of analytical grade and purchased from Beijing Yili Fine Chemical Co. and used as available. Decarbonated deionized water by boiling and bubbling nitrogen is used throughout the experiments.

Preparation of the magnesium ferrite

The magnetic nanoparticles were prepared by a layered precursor method.[28,30] The chemical formula of the as-prepared magnesium ferrite is $MgFe_{1.03}O_{2.54}$ based on ICP analysis and the particle size was estimated to be *ca.* 46 nm upon XRD pattern by Scherrer equation.

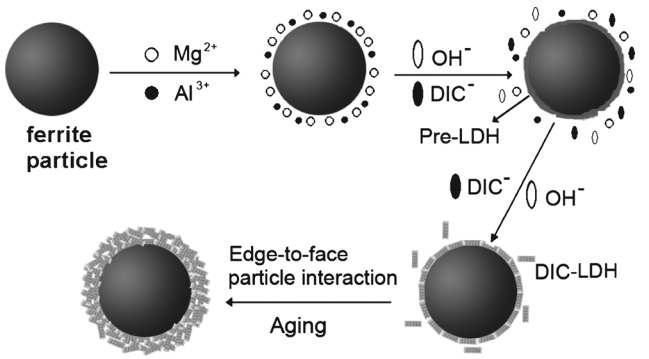

Scheme 1 A schematic representation of the fabrication of the magnetic drug-LDH nanohybrid.

Preparation of the magnetic nanohybrid

The synthesis of the core-shell structural magnetic nanohybrid is described in Scheme 1. In detail, an aqueous solution (100 ml) containing $Mg(NO_3)_2 \cdot 6H_2O$ (5.13 g, 0.02 mol) and $Al(NO_3)_3 \cdot 9H_2O$ (3.75 g, 0.01 mol) was firstly mixed with magnesium ferrite particles with a pre-optimized mass ratio of $Mg(NO_3)_2 \cdot 6H_2O$ to $MgFe_{1.03}O_{2.54}$ of 1:0.05 under ultrasonic vibrations for 20 min resulting in a uniform suspension. Then, a 100 ml aqueous solution of NaOH (4.00 g, 0.1 mol) containing DIC-Na (3.18 g, 0.1 mol) was added dropwise into the suspension with vigorous stirring under an N_2 atmosphere until the final pH was *ca.* 12.8. The resulting slurry was aged at 60 °C for 24 h, centrifuged, washed with decarbonated deionized water and dried at 60 °C under vacuum for 24 h. After magnetic separation to remove the small amount of free drug-LDH particles, the obtained magnetic nanohybrid was denoted as DIC-M. For comparison, the pure DIC-LDH without magnetic substance was prepared using a similar method.

Preparation of the physical mixtures

1.00 g of the obtain DIC-LDH and 0.05 g of the magnetic ferrite particles are mixed by milling method. The resultant was denoted as DIC-Mix. The weight content of the magnetic ferrite in the mixture is 4.76%.

Characterizations

Powder XRD data were taken on a Shimadzu XRD-6000 diffractometer using Cu Kα radiation ($\lambda = 1.5418$ Å, 40 kV, 30 mA). The samples, as unoriented powders, were step-scanned in steps of 0.02° (2θ) in the range 2–70° using a count time of 4s per step. The FT-IR spectra were obtained on a Bruker Vector-22 FT-IR spectrophotometer using a KBr pellet technique (sample/KBr = 1/100). The TEM images were recorded on HITACHI-800 transmission electron microscope. The SEM micrographs were recorded on HITACHI S-4700 field emission scanning electron microscope. The actual metal incorporation contents were measured by inductively coupled plasma (ICP) emission spectroscopy using a Shimadzu ICPS-7500 instrument. CHN microanalysis was carried out using an Elementar Vario Elemental Analyzer. The magnetization of the magnetic nanohybrid was tested on a JSM-13 vibrating-sample magnetometer

at 298 K and ±15kOe applied magnetic field. Determination of the total amount of the intercalated DIC in nanohybrid was measured by dissolving 0.05 g of the nanohybrid in 250 ml dilute hydrochloric acid solution (0.1 mol/L) and then analyzed by using a Shimadzu UV-2501PC spectrophotometer at $\lambda_{max} = 276$ nm.

In vitro release

A solution simulated gastrointestinal and intestinal fluid at pH 7.45 without pancreatine (phosphate buffered solution, Chinese pharmacopoeia 2005) was employed as release medium. The as-synthesized samples (0.05 g) was suspended in 250 ml release medium in a flask and incubated in a water bath at 37 °C with paddle rotation speed of 50 rpm. A sample of 3 ml, which was replaced by a same volume of fresh buffer, was withdrawn at specified time intervals and centrifuged at 12 000 rpm giving a clear supernatant for determining the concentration of DIC using a standard curve of known concentrations of DIC.

In order to investigate the drug release behavior of the magnetic nanohybrid under the magnetic drug targeting operation, a stable magnetic field (MF) of 0.15 Tesla was applied to emulate the magnetic location and magnetically controlled release process (*i.e.* "MF on" mode). The magnet was placed just beside the flask and the position of the magnet relative to the flask was unchangeable during the whole release process. For comparison, the release behavior of DIC-mix was also tested under "MF on" mode.

To investigate the drug release mechanism of the as-prepared magnetic nanohybrid, the drug release data were fitted using four kinetic models.[31–34]

(1) The first-order rate model has been applied to the ion exchange reaction or release process and can be expressed as $\ln(c_t/c_0) = -kt$, where k is the apparent release rate constant, and c_0 and c_t are the amount of DIC in the LDH nanohybrid at release times 0 and t, respectively.

(2) The Bhaskar equation has been applied extensively to the release process where the diffusion through the particle is the rate limiting step and can be expressed as $\ln(c_t/c_0) = -Bt^{0.65}$, where B is the release constant, c_0 and c_t are the same as in model (1).

(3) The modified Freundlich model describes experimental data on ion exchange and diffusion-controlled process using the equation $(c_0 - c_t)/c_0 = kt^b$, where k is the release rate coefficient and b is a constant, c_0 and c_t are the same as in model (1).

(4) The Ritger–Peppas model is generally used to analyze the release profiles of nonswellable and swellable polymers using the equation $F = kt^n$, where F is the fraction mass of drug released at time t, k a rate constant, and n a characteristic exponent related to the mode of transport of the drug. Generally, the F is limited to 0.60, and it can be expanded to 0.85–0.95 only when the aspect ratio of the release matrix is *ca.* 1. In this study, the F is limited to 0.75 as the aspect ratio of drug-LDH nanocrystals is *ca.* 1 (see Table S1†).

Results and discussion

Crystal structure and chemical compositions

The XRD patterns of DIC-M, DIC-LDH, and DIC-Mix are shown in Fig. 1. It can be seen that the magnetic nanohybrid

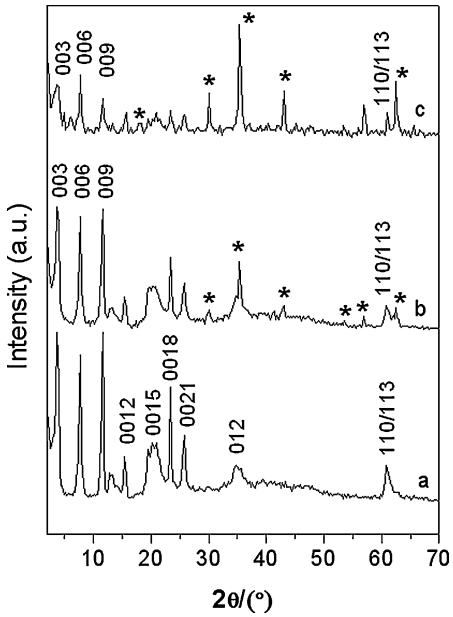

Fig. 1 XRD patterns of (a) DIC-LDH, (b) DIC-M and (c) DIC-Mix. (* magnesium ferrite phase.)

DIC-M presents characteristic reflections of both LDH compound and the magnesium ferrite phase. The three intense peaks at low 2θ angles correspond to diffractions by (003), (006), (009) planes, and one asymmetric peak near 2θ 60° to (110) and (113) planes indexed to the typical hexagonal system LDH compound, while those peaks with * marks are ascribed to the magnesium ferrite phase.[27,28] It is noted that the intensities of the characteristic reflections for both LDH and the ferrite phases in nanohybrid DIC-M are obviously weakened compared to those in pure DIC-LDH and ferrite particles, respectively, indicative of a decrease in LDH crystallinity and plausible coverage for the ferrite particles to some extent. However for the physical mixture DIC-Mix, the characteristic reflections of the magnesium ferrite is quite strong compared to DIC-M though those lines for DIC-LDH is relatively low but still rather sharp, seemingly implying that the both phases existed in DIC-Mix are probably isolated. These phenomena suggest that the DIC-M is not a simple mixture of DIC-LDH with the magnesium ferrite, but a new hybrid composite probably with varied microstructures.

Based upon the lattice parameters derived from the XRD patterns (ESI, Table S1†), the basal spacing d_{003} for pure DIC-LDH is 2.37 nm, a little different from the previously reported values probably due to the different synthesis routes.[4,6] When the magnesium ferrite is involved, the d_{003} of DIC-M is 2.35 nm and the d_{110} is 0.1523 nm, similar to those of the pure DIC-LDH. However, the crystallinity of the LDH phase in the magnetic nanohybrid is much weak compared to the pure DIC-LDH, indicated by the reduced diffraction intensity and increased full width at half-maximum (FWHM) of the (003) and (110) lines. The crystal size in (003) and (110) plane, *i.e.* D_{003} and D_{110} of the LDH particles in DIC-M can be calculated by Scherrer equation ($D = 0.89\lambda/(\beta\cos\theta)$, where λ is the X-ray wavelength, θ the Bragg diffraction angle, and β the FWHM of the XRD lines). It should

be mentioned that the exact evaluation for D_{110} of the LDH particles is carried out through the deconvolution of overlapped (110) and (113) peaks by Original Pro 7.0.[35] As calculated, the D_{110} and D_{003} of the pure DIC-LDH are 19.73 nm and 18.60 nm, while those of DIC-M are obviously reduced, especially for D_{110}, to 14.42 nm and 17.33 nm, respectively. As for DIC-Mix, the d_{003} and D_{110} values are almost the same as those in the pure DIC-LDH. It is quite interesting that the aspect ratio (*i.e.* D_{110}/D_{003}) of the DIC-LDH evidently decreases in the magnetic nanohybrid compared with the pure DIC-LDH and DIC-Mix (Table S1†), suggesting that the introduction of the magnesium ferrite particles obviously hinders the crystal growth of the LDH in the (110) plane, probably due to the orientated-crystallization of the DIC-LDH phase on the surface of the ferrite particles, which will be further discussed later.

The IR spectra of the magnetic nanohybrid and related samples are shown in Fig. 2. The characteristic absorptions between 2000–1000 cm^{-1} for DIC-M, DIC-LDH and DIC-Mix (Fig. 2b–d) are quite similar and characterized as the asymmetric and symmetric stretchings of COO^- group at *ca.* 1577 and 1384 cm^{-1}, respectively.[36,37] The latter one shifts to lower wavenumbers compared to that of raw drug DIC-Na (1400 cm^{-1}) (Fig. 2a) due to the formation of hydrogen bond between COO^- and hydroxyl groups of the Mg–Al layers as often occurred in previously reported drug-LDH systems.[7,28,36] The absorptions at 1533 and 1506 cm^{-1} are assigned to the vibration of benzene ring and 1453 cm^{-1} due to the C–N vibration mode.[36] The strong absorptions at *ca.* 588 cm^{-1} in the magnesium ferrite (Fig. 2e) are attributed to Fe–O lattice vibration mode,[37] which is almost quite weak in DIC-M owing to considerably low content of the ferrite (6.3% in Table S1†). It is noted that the absorptions due to the ferrite are clearly found in DIC-Mix though the ferrite content is even lower (4.7%) than that in DIC-M. The absorptions of the characteristic groups of DIC-LDH in DIC-Mix are exclusively

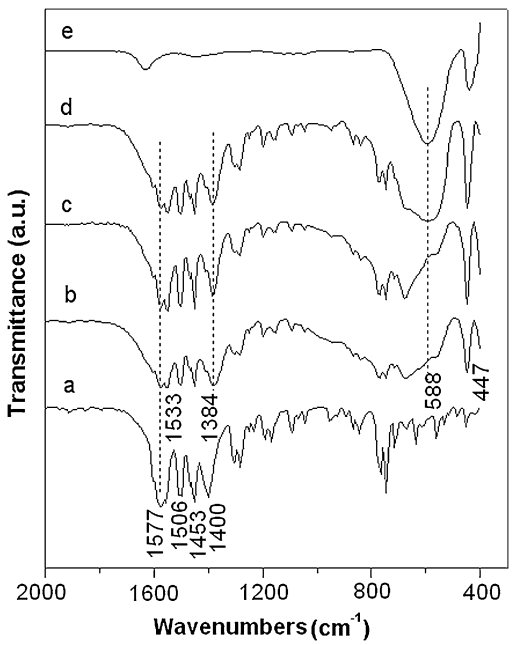

Fig. 2 IR spectra of (a) DIC-Na, (b) DIC-M, (c) DIC-LDH, (d) DIC-Mix and (e) magnesium ferrite.

similar to the pure DIC-LDH, which further confirms that the as-synthesized magnetic drug-LDH nanohybrid is a new nanohybrid probably bearing a core-shell structure, in which the IR absorption of the ferrite is more likely to be shielded by the DIC-LDH coating as proved by later TEM images.

Based on ICP and CHN analysis (Table S1†), the magnetic nanohybrid DIC-M possesses drug loading of 44 wt%, which is a little lower than that of the pure DIC-LDH (52 wt%) and the previously reported,[6] and this is consistent with the slightly reduced layer charge density compared to the pure DIC-LDH.[1,2]

Core-shell structure

Fig. 3 shows the TEM images of the magnesium ferrite, DIC-LDH and DIC-M. Fig. 3a reveals that the magnesium ferrite particles possess approximately spherical morphology with uniform size distribution in 40–60 nm, in accordance with the XRD data on Scherrer equation. Fig. 3b shows approximately hexagonal platelets of the pure DIC-LDH with diameter in the range 40–100 nm with slight aggregation. The difference in the particle sizes obtained from XRD and TEM measurements is most likely due to the stacking of the primary LDH particles. It is also noted that necklace-like linked particles are pictured, being ascribed to the particle–particle interaction.[38] Quite differently, with the magnesium ferrite involved, the particles of hybrid material become larger; while the DIC-LDH cell in the particle has much smaller dimensions than the particles in the bulk DIC-LDH (Fig. 3c). As can be seen, the DIC-M nanoparticles are approximately spherical in shape and well dispersed with diameters of 90–150 nm, though some aggregate particles can be observed. Furthermore, the center of each spherical particle is much darker than the shell, suggesting clearly a core-shell structure of the obtained nanohybrid. The core of this nanohybrid is *ca.* 50 nm in diameter, in good agreement with TEM image of the magnetic core, and the shell is *ca.* 20–40 nm in thickness consisting of much small LDH particles with compact aggregated morphology, evidently different from the morphology of the pure DIC-LDH. In addition, small amount of isolated quasi-hexagonal DIC-LDH platelets can also be observed in DIC-M occasionally.

All of the above results reveal that the introduction of ferrite particles into the drug-LDH hybrid strongly affect the crystal microstructure and crystallinity of the LDH phase. First of all, the ferrite particle can be regarded as heterogeneity in drug-LDH phase, thus the coating of DIC-LDH on the ferrite core is a heterogeneous nucleation and crystal growth process.[39] In this regard, when the magnetic core was introduced into the solution, some of the pre-LDH nuclei[40] would be firstly absorbed on the surface of the magnetic core as described in Scheme 1, and following a crystal growth process. Because of the particle–particle interaction of the LDH nanoparticles,[38] the DIC-LDH nanocrystallites formed in solution tend to be adsorbed on the surface of the magnetic core. As a result, the well formed core-shell structure of the DIC-M is obtained. However, as a heterogeneity, the magnetic core with relatively large size cannot be incorporated readily into the crystal structure of the preformed drug-LDH which is strongly adsorbed onto the surface of the core so as to block the growth active sites of the LDH and the growth rate of the drug-LDH is thus restrained,[39,41] resulting in

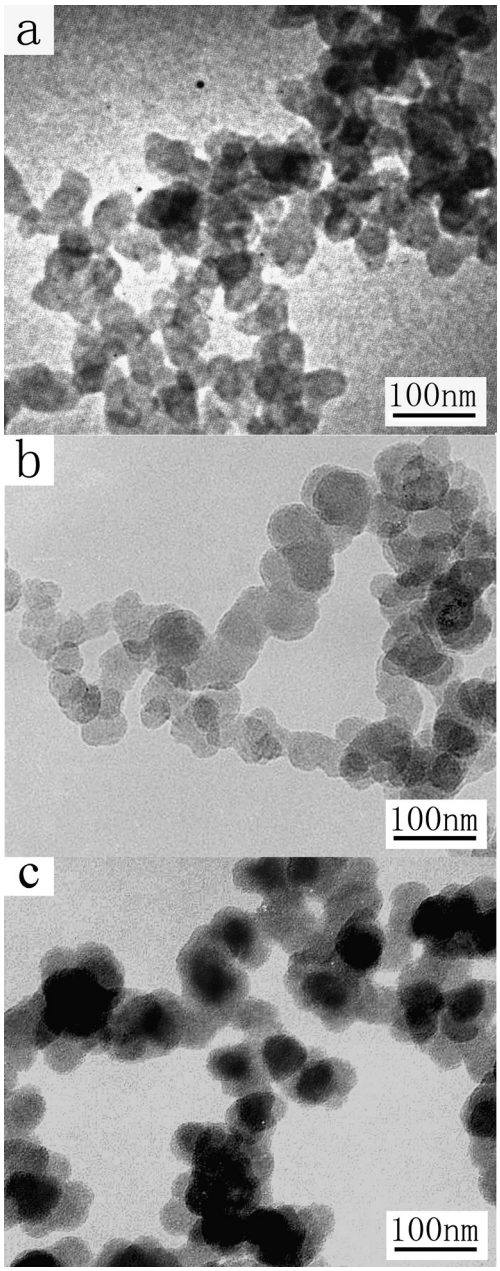

Fig. 3 TEM images of (a) magnetic ferrite, (b) DIC-LDH, and (c) DIC-M.

reduced particle size of the DIC-LDH in the magnetic nanohybrid in present experiment conditions. More importantly, given the semi-rigid property of the LDH layer,[42] the growth of the DIC-LDH crystallites, particularly along the (110) plane, over the spherical surface of the magnetic ferrite particles is profoundly hindered, as demonstrated by the crystal dimension derived by Scherrer equation on XRD data (Table S1†). Further detailed study on formation mechanism of this kind of magnetic nanohybrid is in progress.

Compared to the previous report on the 5-ASA-ZnAl-LDH/$MgFe_2O_4$ system,[28] the present DIC-M exhibits a much clearer core-shell structure and well dispersed properties. Moreover, the particle size of the DIC-M meets the requirement for administration by injection and makes these magnetic nanohybrids an effective drug carrier for magnetic drug targeting.[33] It must be stressed that virtually any chemotherapeutic agent that can be intercalated into the LDH matrix may be successfully entrapped within this magnetic nanohybrid, giving it a broad potential range of utility.

The magnetic-sensitive behavior

The magnetic property measurement of the magnetic nanohybrid at room temperature by using VSM is depicted in Fig. 4a. The saturation magnetization value of the DIC-M is 5.54 emu/g, much lower than that of the magnesium ferrite (28.93 emu/g), which is attributed mainly to the contribution of the volume of non-magnetic coating to the total sample. Additionally, the non-magnetic coating layer can be considered as a magnetically inert layer on the surface of a magnetic core.[28] The magnetic separability of such magnetic nanohybrids was tested in ethanol by placing a magnet near the flask. The yellow particles in solution were attracted towards the magnet within 20 s (Fig. 4b), directly demonstrating the strong magnetic sensitivity of the magnetic nanohybrid, hence providing an easy and efficient way to separate DIC-M particles from a sol or a suspension system and to carry drugs to the targeted locations under an external magnetic field.

Magnetically controlled drug release

Based on above discussions, it can be safely deduced that the microstructure of the magnetic nanohybrid is evidently affected by the introduction of the magnetic ferrite. Such an alteration of microstructure in the magnetic hybrid may result in its dissimilar release behavior, especially under an external magnetic field. In this respect, the magnetically controlled drug release of DIC from DIC-M under "MF on" and "MF off" operations at 37 °C is investigated and the results are presented in Fig. 5. For comparison, the release profiles of the pure DIC-LDH and the DIC-Mix are also presented. As can be seen, all the release profiles show a fast release rate at the beginning followed by a slower one with increased time until the equilibrium is attained, as in the case often observed in the drug-LDH intercalates.[6,7,32,33]

Interestingly, the DIC-M under "MF off" mode shows obviously faster release rate of DIC than the pure DIC-LDH. In detail for DIC-LDH, the $t_{0.5}$ (the time for release fraction of 50%) is 45 min with a burst release (the release fraction in the initial 2 min) of 22.1%, while ~80% of DIC was released after 7 h. For the core-shell structured DIC-M, the $t_{0.5}$ decreases to 25 min with a burst release of 28.2%, and about 82% of DIC was released in 4.5 h. These results clearly suggest that the release rate of DIC-M is faster than DIC-LDH, which can be reasonably ascribed to the much smaller particle size of the coated DIC-LDH particles in DIC-M.[6,33] However, the release profile of DIC-Mix and its release parameters are quite similar to those of pure DIC-LDH, providing an indirect evidence for DIC-Mix being of a simple mixture of DIC-LDH and the ferrite particles as implied by the XRD and IR analysis.

Quite differently, the release profile of DIC from DIC-M under the "MF on" mode reveals a $t_{0.5}$ of 60 min and an equilibrium release percentage of merely 84% over more than 16 h,

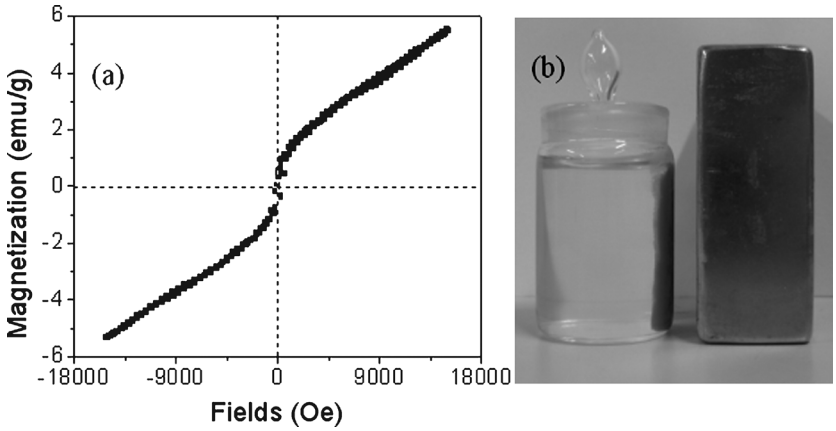

Fig. 4 The magnetic properties of DIC-M: (a) room temperature magnetization curve, and (b) separation from solution under an external magnetic field reflecting strong magnetic response.

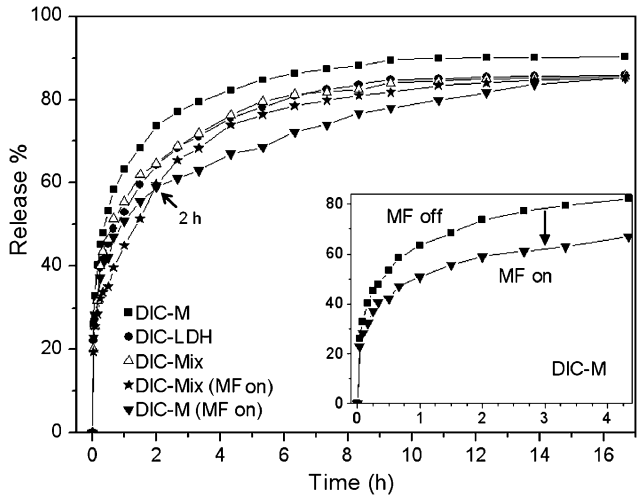

Fig. 5 Release profiles of DIC from the DIC-M, DIC-LDH and the DIC-Mix in pH 7.45 PBS. The insert shows the release profiles of DIC-M with and without an external magnetic field ("MF on" and "MF off", respectively).

showing a dramatically slower release rate than that for "MF off" mode. A similar phenomenon on magnetic sponge-like hydrogel systems has been previously reported by Liu *et al.*[25,26] Over a time span of 5 h, the released amount of only 66% under "MF on" mode is evidently small compared to that of 85% under "MF off" mode. These findings strongly indicate that the applied magnetic field effectively retarded the drug release from the magnetic nanohybrid. The inset in Fig. 5 specifically reflects a little lower burst release of ~20%, illustrating that the release profile at the very beginning is also differentiated from that under "MF off" mode. Very interestingly, the release profile of DIC-mix under "MF on" mode (Fig. 5) apparently shows an even slower release rate than DIC-M after initial burst release, which can be ascribed to a synergetic effect from the larger particle size of pure DIC-LDH and a possible encapsulation in aggregates of the magnesium ferrite particles. However after 2 h, the profile tends to be identical to that of pure DIC-LDH actually due to its physical mixing nature.

To understand the release mechanism of the drug molecules from the magnetic nanohybrid, four kinetic models are employed to fit the measured data (Fig. 6) and the rate constants and the r^2 values obtained from the fits are given in the ESI, Table S2.† The first-order kinetic model gave r^2 of 0.8471 and 0.9324 for the release profile of DIC-M under "MF off" and "MF on" modes, respectively, suggesting that this model is not suitable for explaining the whole release behavior of DIC-M. The Bhaskar equation gives r^2 of 0.9769 for the release profile under "MF off" mode, indicating that the release of DIC from DIC-M is a particle diffusion controlled process similar to the previous report.[6] A detailed examination of the data point distribution suggests that the whole release process for DIC-M consists of two linear stages, though a high r^2 value was obtained, probably owing to the much small particle size of the coated DIC-LDH crystallites and the aggregation of the DIC-LDH nanoparticles on the surface of the magnetic core. Smaller particles with less regular shape can provide more available side edges/surfaces[33] and a shorter diffusion path length which may result in a high amount of burst release and fast release in the first stage, while the aggregation of the coated DIC-LDH particles would lead to a longer diffusion path length and higher diffusion resistance in the magnetic nanohybrid resulting in the slower release in the second stage.[43] When the external magnetic field was applied, these two stage release features become more pronounced, indicative of an evident retardation for drug molecules to diffuse through the magnetic nanohybrid particles, more likely due to the aggregation of the magnetic nanohybrid particles induced by an applied external magnetic force.

Furthermore, the modified Freundlich equation and the Ritger-Peppas model provide reasonable r^2 values of more than 0.9922 for the release profiles of DIC-M under both "MF on" and "MF off" modes. The fitting results for the release under "MF on" mode show much lower k and n values than those under "MF off" mode (Table S2†), providing direct evidence of the magnetically-induced inhibition effect on drug molecular diffusion. It is given that the modified Freundlich model describes the release behavior from the flat surface with the heterogeneous sites by ion exchange diffusion process,[32,33] while the Ritger-Peppas model was proposed to describe the release behavior of nonswellable and swellable polymer-based drug

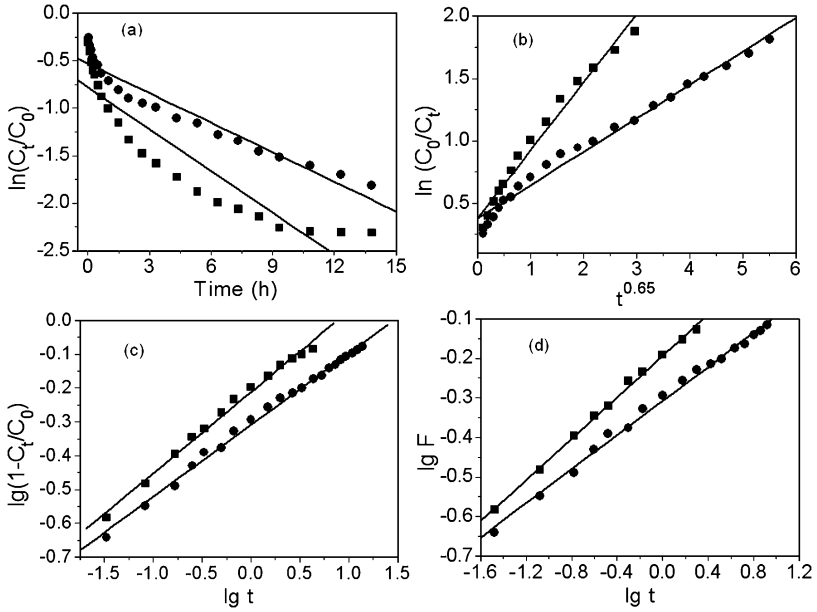

Fig. 6 Plots of kinetic models of (a) first-order kinetic model, (b) Bhaskar equation, (c) modified Freundlich model, and (d) Ritger-Peppas model for the release of DIC from DIC-M under "MF on" mode (■) and "MF off" mode (●).

delivery systems.[34,44] More recently, Hu *et al.*[26] employed the Ritger-Peppas model to describe vitamin B12 release from "magnetic nanoparticles" under an external magnetic field. We noticed that the modified Freundlich model actually gives the same mathematical expression as the Ritger-Peppas one despite their different originating source from varied release systems.[32–34] In fact, both models give good fitting data for the release profiles of DIC-M under both "MF on" and "MF off" modes (Fig. 6 and Table S2†). The fitting data from the modified Freundlich model imply that the release profiles of DIC-M under both modes belong to a kind of heterogeneous diffusion processes, while that from Ritger-Peppas model plausibly reveal that the present magnetic nanohybrid may possess a polymer-like structural morphology and more than one diffusion types are involved in the drug release process. Undoubtedly, quite consistent explanation is obtained from both models. It is noted that the diffusion exponent n derived from Ritger-Peppas model is small and out of the given n values range in Ritger-Peppas model, which can be ascribed to a relatively high burst release at initial stage and a much slow release process in the long time.[34] To the best of our knowledge, there is no report on using Ritger-Peppas model to effectively analyze drug release behavior of drug-LDH systems so far, and the present study may be an extensibility of the application of Ritger-Peppas model. The obtained positive results seemingly imply a plausible linkage existed between the polymer-based and layered inorganic clay-based drug delivery systems upon the present novel magnetic drug-LDH nanohybrid composites.

Further SEM determinations (Fig. 7) show relatively direct supporting evidence. Clear hexagonal nanocrystals with sharp edge of the pure DIC-LDH could be observed by SEM (Fig. 7a) as noted in above TEM image, while for DIC-M, besides the evidently smaller particle size, the hexagonal LDH nanocrystals are scarcely perceived and approximately spherical and a little surface roughed particles are displayed (Fig. 7b). Being treated

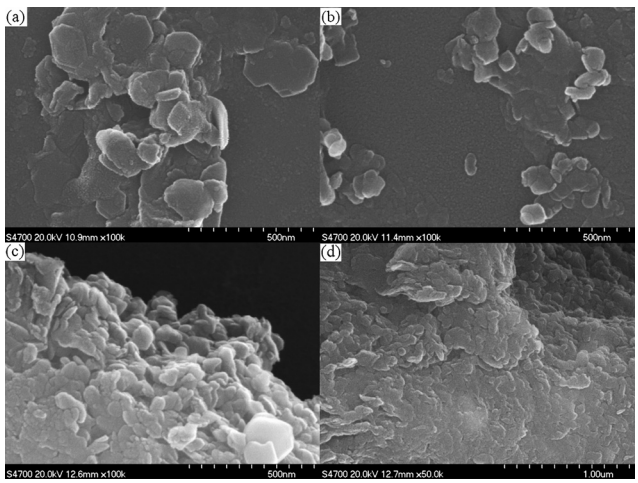

Fig. 7 SEM images of DIC-LDH (a), as-prepared DIC-M (b) and the DIC-M sample treated under external magnetic field (0.15 T) for 30 min (c and d).

with external magnetic field for DIC-M, the most distinguished difference is a strong aggregation of the magnetic nanohybrid particles triggered by an external magnetic force, which result in a gel-like aggregation of DIC-M particles (Fig. 7c and d), hence reasonably result in another longer diffusion path, and may further slower the release rate of the DIC from DIC-M.

Based on the above analyses, a microstructure-dependent drug release mechanism for the magnetic nanohybrid is proposed and schematically presented in Fig. 8. It can be seen that the magnetic nanohybrid particles are well dispersed in the release media under "MF off" mode with constant shaking operation, and the release of DIC molecules from the magnetic nanohybrids is mainly controlled *via* the interlayer intraparticle diffusion between the LDH layers (referred as path I in Fig. 8) and

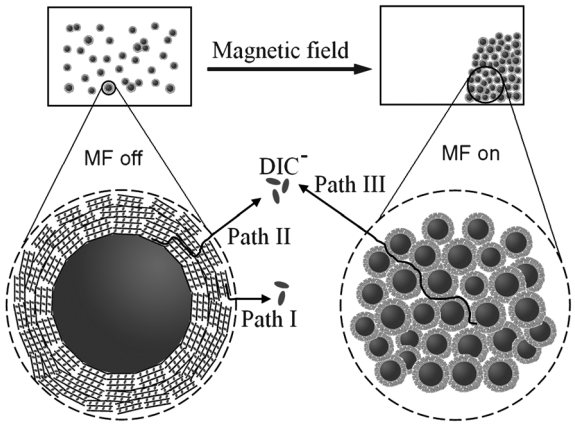

Fig. 8 A schematic drawing of DIC release from the core-shell structured nanohybrid composites with and without an external magnetic field.

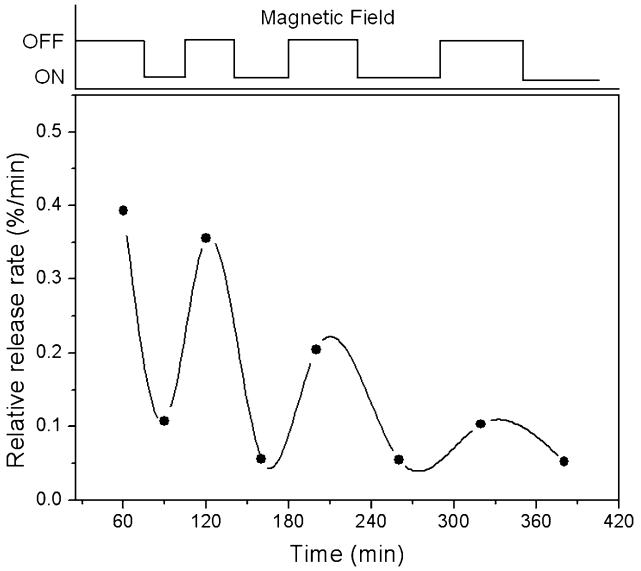

Fig. 9 The relative drug release rates of the magnetic drug-LDH DIC-M nanoparticles under repeated MF on-off operations.

interparticle diffusion among the stacking DIC-LDH nanoparticles coated on the surface of the magnetic cores (path II in Fig. 8). While under "MF on" mode, the magnetic nanohybrid particles are aggregated extensively owing to the non-contact magnetic force. Consequently, besides the above two diffusion paths, the interparticle diffusion among the soundly aggregated magnetic nanoparticles induced by the magnetization significantly affect the drug release properties of the DIC-M, due to the even longer diffusion path length and higher diffusion resistance, particularly for the DIC molecules entrapped in deep interior part of the aggregates (path III in Fig. 8), while the initial release owing to the outside parts of the aggregates is less affected under "MF on" mode as indicated in Fig. 5. Therefore, a considerably decreased drug release rate was induced after initial fast release, and the release constant k obtained from kinetic fitting was reasonably reduced (Table S2†). These results are in accordance with the slower release feature observed for DIC-M under "MF on" mode rather than those for DIC-M under "MF off" and the pure DIC-LDH. From this point, the magnetic nanohybrid not only renders these kind of magnetic drug delivery systems a targeting location function, but also slow/sustained drug release properties with proper external magnetic field employed through synergetic interactions of the above-mentioned three diffusion paths.

An alternative change in the drug release rate of DIC-M can also be identified (Fig. 9) under a consecutive MF on-off operation. The cumulative drug-release amount decreased with "MF on" and increased to some extent again under "MF off". This tunable release rate further substantiates the rearrangement of the magnetic nanoparticles due to the magnetic force induced aggregation and this also indicates a potential use of this kind of novel magnetic supramolecular drug-LDH nanohybrid for an in-time drug release.[23] Elastic fatigue behavior is also observed, probably due to the lower concentration of the ferrite in the hybrid, further properly increasing the amount of ferrite maybe possible for better anti-fatigue properties. This is the first observation of an elastically magnetically controlled switch-on property for the drug release to some extent from the magnetic drug-inorganic layered nanohybrid systems similar to the previously reported magnetic-sensitive silica nanospheres[23] and ferrosponge system.[25,26] Work on magnetic drug-LDH nanohybrids involving other non-steroid anti-inflammatory drugs and anticancer agents is in progress.

Conclusion

In conclusion, a new magnetic nanohybrid with a core-shell structure is assembled by a one step coprecipitation method. The DIC-LDH is coated on the surface of the magnesium ferrite core to produce a magnetic nanohybrid with particle size ranging from 90 to 150 nm. The coated DIC-LDH crystallites present a much smaller particle size compared to that of the pure DIC-LDH due to the prohibition effect of the magnetic core to the growth of the LDH crystallite. The drug release without a magnetic field shows that the drug release rates of the magnetic nanohybrid increase significantly compared to that of the DIC-LDH due to the much smaller particle size. On the contrary, drug release with a magnetic field reveals that the drug release rates of the magnetic nanohybrid decrease dramatically due to the aggregation of the magnetic nanohybrid particles. Based on the release data fitting and the SEM results of the DIC-M, a microstructure-dependent drug release mechanism of the magnetic nanohybrid is proposed. More importantly, the magnetic nanohybrid exhibits an obvious pulsatile drug release property under a consecutive MF on-off operation, giving it a possible application in an in-time drug release mechanism. In addition, this nanohybrid has strong magnetization response and proper particle size for administration by injection. Therefore, we expect this magnetic nanohybrid may be applicable in magnetic drug targeting.

Acknowledgements

The work was supported by the National Nature Science Foundation of China (No. 20776012 and Key20531010), Program for Changjiang Scholars and Innovative research Team in University (IRT0406), 111 Project (No. B07004) and National Basic Research 973 program (2009CB939802).

References

1 F. Cavani, F. Trifirò and A. Vaccari, *Catal. Today*, 1991, **11**, 173.
2 D. G. Evans and X. Duan, *Chem. Commun.*, 2006, 485.
3 J. H. Choy, S. J. Choi, J. M. Oh and T. Park, *Appl. Clay Sci.*, 2007, **36**, 122.
4 A. I. Khan, L. X. Lei, A. J. Norquist and D. O'Hare, *Chem. Commun.*, 2001, 2342.
5 J. H. Choy, S. Y. kewk, Y. J. Jeong and J. S. Park, *Angew. Chem., Int. Ed.*, 2000, **39**, 4041.
6 V. Ambrogi, G. Fardella, G. Grandolini, L. Perioli and M. C. Tiralti, *AAPS PharmSciTech*, 2002, 3.
7 H. Zhang, K. Zou, S. Guo and X. Duan, *J. Solid State Chem.*, 2006, **179**, 1791.
8 K. J. Widder, A. E. Senyei and D. G. Scarpelli, *Proc. Soc. EXP. Biol. Med.*, 1978, **58**, 141.
9 V. P. Torchilin, *Eur. J. Pharm. Sci.*, 2000, **11**(Suppl. 2), S81.
10 A. S. Lübbe, M.D. Ph. D., C. Alexiou and C. Bergemanm, *J. Surg. Res.*, 2001, **95**, 200.
11 Q. A. Pankhurst, J. Connolly, S. K. Jones and J. Dobson, *J. Phys. D: Appl. Phys.*, 2003, **36**, R167.
12 S. Mornet, S. Vasseur, F. Grasset and E. Duguet, *J. Mater. Chem.*, 2004, **14**, 2161.
13 A. K. Gupta and M. Gupta, *Biomaterials*, 2005, **26**, 3995.
14 A. S. Lübbe, C. Bergemann, H. Riess, F. Schriever, P. Reichardt, K. Possinger, M. Matthias, B. Dorken, F. Herrinann, R. Gurtler, P. Hohenberger, N. Haas, R. Sohr, B. Sander, A. Lemke, D. Ohlendorf, W. Huhnt and D. Huhn, *Cancer Res.*, 1996, **56**, 4686.
15 J. Fortin-Ripoche, M. S. Martina, F. Gazeau, C. Menager, C. Wilhelm, J. Bacri, S. Lesieur and O. Clement, *Radiology*, 2006, **239**, 415.
16 J. L. Arias, M. A. Ruiz, V. Gallardo and Á. V. Delgado, *J. Control. Rel.*, 2008, **125**, 50.
17 J. Xie, K. Chen, H.-Y. Lee, C. Xu, A. R. Hsu, S. Peng, X. Chen and S. Sun, *J. Am. Chem. Soc.*, 2008, **130**, 7542.
18 S. Goodwin, C. Peterson, C. Hoh and C. Bittner, *J. Magn. Magn. Mater.*, 1999, **194**, 132.
19 W. R. Zhao, J. L. Gu, L. X. Zhang, H. R. Chen and J. L. Shi, *J. Am. Chem. Soc.*, 2005, **127**, 8916.
20 S. H. Wang, X. Shi, M. Van Antwerp, Z. Cao, S. D. Swanson, X. Bi and J. R. Baker, Jr., *Adv. Funct. Mater.*, 2007, **17**, 3043.
21 X. Shi, S. H. Wang, S. D. Swanson, S. Ge, Z. Cao, M. E. Van Antwerp, K. J. Landmark and J. R. Baker, Jr., *Adv. Mater.*, 2008, **20**, 1671.
22 E. R. Edelman, J. Kost, H. Bobeck and R. Langer, *J. Biomed. Mater. Res.*, 1985, **19**, 67.
23 S. H. Hu, T. Y. Liu, D. M. Liu and S. Y. Chen, *Langmuir*, 2008, **24**, 239.
24 M. D. P. Vania, H. D. P. L. Silvia, S. Leonard, I. Bruce, R. Zeev and R. Nitsa, *Langmuir*, 2006, **22**, 5894.
25 T. Y. Liu, S. H. Hu, T. Y. Liu, D. M. Liu and S. Y. Chen, *Langmuir*, 2006, **22**, 5974.
26 S. H. Hu, T. Y. Liu, D. M. Liu and S. Y. Chen, *J. Control. Rel.*, 2007, **121**, 181.
27 H. Zhang, R. Qi, D. G. Evans and X. Duan, *J. Solid State Chem.*, 2004, **177**, 772.
28 H. Zhang, K. Zou, H. Sun and X. Duan, *J. Solid State Chem.*, 2005, **178**, 3485.
29 G. Carja, H. Chiriac and N. Lupu, *J. Magn. Magn. Mater.*, 2007, **311**, 26.
30 J. J. Liu, F. Li, D. G. Evans and X. Duan, *Chem. Commun.*, 2003, 542.
31 R. Bhaskar, R. S. R. Murthy, B. D. Miglani and K. Viswanathan, *Int. J. Pharm.*, 1986, **28**, 59.
32 J. H. Yang, Y. S. Han, M. Park, T. Park, S. J. Hwang and J. H. Choy, *Chem. Mater.*, 2007, **19**, 2679.
33 Z. Gu, A. C. Thomas, Z. P. Xu, J. H. Campbell and G. Q. Lu, *Chem. Mater.*, 2008, **20**, 3715.
34 P. L. Ritger and N. A. Peppas, *J. Control. Rel.*, 1987, **5**, 23.
35 Z. P. Xu and H. C. Zeng, *J. Phys. Chem. B*, 2001, **105**, 1743.
36 L. Mohanambe and S. Vasudevan, *J. Phys. Chem. B*, 2005, **109**, 15651.
37 K. Nakamoto, in *Infrared and Raman Spectra of Inorganic and Coordination Compounds*, John Wiley and Sons, New York, 5th edn, 1997.
38 J. A. Gursky, S. D. Blough, C. Luna, C. Gomez, A. N. Luevano and E. A. Gardner, *J. Am. Chem. Soc.*, 2006, **128**, 8376.
39 R. B. Corey, in *Adsorption of Inorganics at Solid-Liquid Interfaces*, ed. M. A. Anderson and A. J. Rubin, Ann Arbor Science, Michigan, 1981, pp. 161–179.
40 Z. P. Xu and G. Q. Lu, *Chem. Mater.*, 2005, **17**, 1055.
41 P. Hartman, in *Crystal growth*, ed. P. Hartman, Elsevier North-Holland, New York, 1973, pp. 390–392.
42 D. R. Hines and S. A. Solin, *Phys. Rev. B*, 2000, **61**, 11348.
43 P. Gunawan and R. Xu, *J. Pharm. Sci.*, 2008, **97**, 4367.
44 P. L. Ritger and N. A. Peppas, *J. Control. Rel.*, 1987, **5**, 37.